A Metrology Development Platform for Digital Image Correlation-Based Measurement of Thermal Expansion and Cure Shrinkage in Epoxies

Alexander K. Landauer
National Institute of Standards and Technology
Gaithersburg, MD, USA
alexander.landauer@nist.gov
0000-0003-2863-039X

***Abstract*—NIST is developing a suite of material metrology tools to understand and characterize the development of residual stresses during epoxy curing. In this work, the application of digital image correlation (DIC)-based metrology for coefficient of thermal expansion (CTE) and (effective) cure shrinkage (E)CS is described. The DIC setup and experimental considerations are explained in detail. An example analysis of CTE for a prototype test material, also under development, is discussed with example CTE data shown. This contribution helps the interested reader to understand the basic design decisions for establishing DIC-based metrology for epoxy cure, and future developments may include robotic calibration, humidity control and epoxy confinement.**

Keywords—epoxy packaging, digital image correlation, cure shrinkage, coefficient of thermal expansion

I. Introduction

The increasing complexity of chip assemblies as the semiconductor industry moves toward 3D heterogeneous architectures has led to increased introduction of sophisticated epoxies into build ups [1]. With such a substantial use of epoxy, quantifying thermo-chemo-mechanical properties such as (effective) cure shrinkage [(E)CS] and coefficient of thermal expansion (CTE) is an important step for developing predictive models of these systems. Mechanical properties such as strength, toughness, and adhesion are important primary performance measures, but calibrated CS and CTE mismatch are important parameters for informing models to predict warpage and other downstream challenges [2-4]. Here, the focus is on a development platform for digital image correlation (DIC)-based metrology for quantification of (E)CS and CTE, which can be used to study *in situ* curing.

Digital image correlation-based techniques have been applied to measure CS, CTE, and similar properties in various previous works, e.g., [5-9]. Package warpage is also characterized with DIC and it is recognized as a possible approach for package warpage measurement by JEDEC standard JESD22-B112C [10-11]. Commercial instruments utilizing DIC for displacement and strain measurements are available from packaging metrology companies [3]. Several DIC vendors have been commissioned or sell specialized systems for measuring package warpages and packaging materials with DIC. Since the use of DIC for these measurements is becoming widespread, this project aims to democratize access, explore the potential of the technique, and provide insight into the metrological details.

To address the multifaceted characterization needs for packing epoxies a suite of test methods is under development by a broader project team at the National Institute of Standards and Technology (NIST) [12]. These test methods encompass a wide range of chemical, thermal, and mechanical assays from molecular-scale to part-scale. The DIC system that is the focus of this work, shown in Fig. 1, embodies one of the tools in this suite, which was briefly discussed in Centellas *et al*. [12]. This project focuses on describing development of the DIC platform, exploring challenges, and discussing methodologies for the system to quantify (E)CS and CTE with sufficient fidelity and with *in situ* capabilities to inform reliable predictive models. Using a simple, well-controlled test material as a baseline, this work discusses the application of this DIC system to (E)CS and CTE measurements. Since both measurements are similar, the example application highlighted focuses on CTE measurement and changes to the methodology needed for (E)CS are noted.

II. Experimental

A. Material

A prototype test material (TM01) under development by colleagues at NIST is used as the example case for the remainder of this paper. This is a highly simplified model material of an underfill-like epoxy. It consists of bisphenol F epoxy resin cured with diethyl toluene diamine, which are constituents foundational to advanced underfill formulations. Notably, no additional modification agents or fillers are included in this formulation. After formulation, the material is stored at about 4 °C in a lab refrigerator until about 20 min before use.

B. Specimen Design and Fabrication

For (E)CS and CTE measurements with DIC, specimen design and fabrication are critical to measure meaningful, representative data on the material behavior. DIC is a noncontact surface-type measurement in contrast to, e.g., fiber

This work was performed with funding from the CHIPS Metrology Program, part of CHIPS for America, National Institute of Standards and Technology, U.S. Department of Commerce. National Institute of Standards and Technology Award # 70NANB24H283.

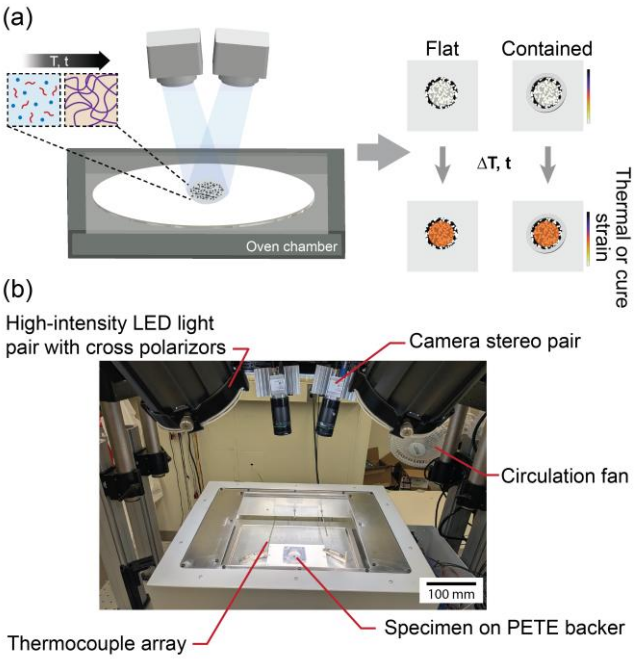

Fig. 1 Diagrams of the setups. (a) Sketch of the DIC and oven system used for curing (cure shrinkage measurement) and CTE measurement, with the DIC region of interest highlighted. (b) Annotated photograph of the oven and DIC setup in lab. Camera triggering, acquisition computer, and oven controller are not shown.

Bragg [13], [14] or TMA [3] experiments where a sensor is touching or embedded into the material. A relatively small quantity of material (ca. 50 mg) is sufficient for (E)CS and CTE measurements for this DIC method. To decouple the specimen from a stiff backer, which could influence the total strain response after the material passes its gelation point, a thin and relatively compliant high-temperature polymer backer sheet is used. Depending on the material under study and thermal profile different backer sheet polymers are needed. In our previous work, a nominally 0.02 mm polyetherimide (PEI) sheet was used effectively [12]. For TM01, the low surface free energy and hydrophilic nature of the PEI resulted in flow of the TM01 during curing. Instead, a high-temperature polyethylene terephthalate (PETE) sheet (ca. 0.03 mm) was used for this study. This provided a surface on which the liquid epoxy beaded during the transient low viscosity portion of curing, i.e., when at elevated temperature with low degree cure.

After synthesis of the prepolymer, it is stored in a laboratory refrigerator until about 5 min before use. Preliminary data indicates that moisture uptake in the epoxy during long term (i.e., more than four weeks) storage of prepolymer or cured resin may affect characteristics such as CTE, residual stress, and viscoelastic moduli. Thus, specimens for the example data shown were fabricated within three weeks of synthesis, cured within 30 min of fabrication, and tested within five days of curing. To make a specimen, an approximately 5 cm by 5 cm square of the selected backer material is cut from the as-received material. Depending on the viscosity evolution during cure and surface interaction of the epoxy and backer, a 3D printed die mold can be used to press a containment feature into the backer. For the example TM01 experiments a die with a 7 mm inner diameter, 11 mm outer diameter, and 2 mm tall ridge was used to press a containment feature into the backer. During cure the PETE relaxes this plastic strain, and it re-flattens. However, in conjunction with the surface energy effects, it is sufficient to produce a suitability repeatable geometry for CTE measurement. This strain relaxation disrupts quantitative determination of the stress onset during cure for (E)CS measurements, and thus the containment feature may not be suitable when adopting this approach. Once the backer is prepared, a scoopula is used to deposit a drop of the prepolymer on the backer. This is typically 40 mg to 45 mg of material. For the (E)CS experiments the specimens are speckled (see Sect. II.D.), then cured (see Sect. II.C.) while collecting DIC data on both the specimen and the surrounding backer. For the CTE measurements, the specimens are cured prior to speckling (in this case using the same oven as DIC), speckled, left at lab temperature (ca. 22 °C) for the paint to dry overnight, then placed in the oven for temperature cycling.

C. Oven Design and Temperature Schedules

The oven used for environmental control is based on a modified conduction/convection commercially available reflow oven as model GF-C2 from DDM NovaStar Inc. The original viewing window was replaced with a single pane antireflective coated window approximately 300 mm square. A four-sensor stainless steel-enclosed ungrounded K-type thermocouple array (TMP41xx, Phidgets Inc) was added to monitor temperature in multiple locations, as shown in Fig. 1b. Calibrations for the example data shown here were conducted with the lid open. A programmable, computer interfaced oven controller was installed, allowing for control of heating rate and development and implementation of temperature control schedules. An office fan is installed above the viewing window to minimize schlieren effects associated with refractive index changes in the air.

Several nominal temperature-controlled curing schedules have been applied to understand the cure behavior of this material. In the example case of CTE measurement used here a specimen cure at 120 °C for 8 h with heating ramp at 5 °C/min and cooling at the natural rate of the oven is used. For the example post-cure CTE measurements, specimens are heated from nominal room temperature (25 °C) held at 40 °C for 5 min, then heated at 3 °C/min to 75 °C, held for 5 min, allowed to cool at the natural rate of the oven to 40 °C, held for 5 min, and cycled this way twice more (see Fig. 2c *inset*). Preliminary measurements conducted by a collaborator using a stress bench measurement based on the instrument described in [12] showed linear behavior for the range 25 °C to 150 °C, thus for the examples used here a limited range is used.

D. Speckle Patterning

Creating high-quality speckle patterns is a challenge, sometimes considered an art rather than science, of DIC metrology. Many solutions are available, and techniques vary depending on the wide range of material on which DIC is applied. For more details and information on DIC pattern

optimization, refer to the DIC Good Practices Guide [15]. In previous work with a commercial glob top material a basic spray painting technique was successful, since the material was well-behaved and colored an opaque black [12]. In contrast, the TM is specifically formulated to have minimal added components and thus requires more careful handling. In addition, the material is a transparent yellow color, making speckling more challenging.

For the cure shrinkage measurement speckling must be conducted when the material is uncured to perform DIC measurements during the cure process. For the CTE measurement speckling is conducted after curing and cooling to room temperature. Since the material and backer sheets are translucent, black speckles are used, and the specimen is placed on a flat, aluminum test plate in the oven which is painted a uniform, flat white with spray paint. Prior to any testing, the spray-painted aluminum plate is baked at a temperature above the maximum test temperature for at least 10 min to reduce the risk of off-gassing interfering with the cure process. A challenge of this approach is that any gap between the backer and white plate causes speckle shadows that corrupt the measurement – for the glob top material this was not a concern, but for the TM01 this is a challenge since the containment feature creates such a gap. For the TM01 measurements this is mitigated since the backer is translucent and speckle shadows are not apparent in the images (see, e.g., Fig. 2a).

For speckles themselves, after trials with a series of speckle options, an acrylic ink applied with an airbrush seems to be the most successful. The solvent carrier in spray-paints was miscible with the prepolymer causing streaky, inconsistent patterns and concerns about contamination disrupting cure. Graphite or toner particles dusted on the surface clumped and did not adhere well to the backers. The acrylic ink seems immiscible creating relatively uniform dot size patterns and reducing concerns about contamination. By tuning the airbrush pressure and nozzle opening the resultant dot can be optimized for the lenses and resolution of the camera system to yield approximately 4 px to 7 px speckles of the desired density. Since the backer material is a thin sheet, airflow from the brush can easily disrupt patterning. A straightforward solution is to use cellophane tape on the corners of the backer to adhere them to a quarter sheet of paper. Once a suitable pattern has been achieved and the paint has dried, the specimen is ready to place in the oven. Airflow from convection in the oven can also cause similar issues during the experiment. For the CTE example, an aluminum ring with an inner diameter of approximately 30 mm is placed on the backer sheet to gently restrain it for the duration of testing.

E. DIC Hardware

The stereo-DIC system consists of two cameras with lenses, two studio lights, and synchronization and data acquisition hardware (synchronization and trigger hardware were purchased from MatchID Inc.). The camera pair consists of two 24.4 MPx cameras (ace2 a2A5328-15umPRO Monochrome, Basler AG) with 50 mm lenses (Fujinon CF50ZA1S, Fujifilm Corp.; set to f/4) and linear polarizing filters. They are mounted in a rigid frame to the same optical table as, and above, the oven (see Fig. 1b), with stereo angle -14.85° and stand-off about 430 mm. Each camera is passively cooled with an aluminum radiator, and cameras are started 30 or more minutes prior to the experiment to minimize thermal warpage artifacts in the sensor [15]. The cameras are synchronized and triggered with a data acquisition system.

Cross-polarized lighting is provided from two high-intensity Light Emitting Diode (LED) studio lights mounted to the same frame as the cameras (see Fig. 1b) with custom linear polarizers constructed from linearly polarizing film in a 3D printed rotational mount. While the cross-polarized configuration significantly reduces available light, it also dramatically reduces specular reflections that tend to saturate the sensor in hotspots without providing useful data, especially on the smooth, shiny surface of the epoxy specimen [16].

F. Data collection

Prior to collecting data, the intrinsic and extrinsic camera and stereo parameters are calibrated. For the example data for TM01 CTE the calibration was conducted using the software vendor-provided (MatchID Inc.) calibration package. A 9 dot by 12 dot ceramic calibration target with 2.5 mm spacing is used. This calibration corrects for lens distortions (radial, tangential, polynomial) and uses a noncentral optical raytracing model. For other DIC packages different calibration targets and routines were used as needed.

For a given specimen, parameters such as exposure, sensor cropping, and frequency are selected to optimize the measurement (see, e.g., [15]). This yielded images of about 1500 px by 1300 px, exposure around 5000 µs, and frame rate of 0.2 Hz. Images were filtered with light Gaussian blur (5 px width, 1 sigma) to reduce speckle aliasing. The image collection was started with several frames of nominally static images for noise floor assessment. To perform an experiment, the oven profile, image collection, and thermocouple data capture are started with ca. 5 s of each other and in post-processing are assumed to have been simultaneous. This introduces a negligible timing error (ca. 5 s) to the overall experiment (ca. 4 h of data collection).

Thermocouples were sampled at 5000 ms with an 11-point low pass filter using the vendor-provided data acquisition software (Phidgets Inc.). This resulted in about 3400 time points per experiment. For primary temperature data, a thermocouple clamped to the aluminum test plate is used. Under nominally isothermal conditions the noise floor for the thermocouple (one standard deviation) is approximately 0.08 °C. A comparatively large bias error is likely present due to the location of the temperature probe compared to the sample. In future improvement to the oven design, the sensor will be embedded in the aluminum test plate immediately below the specimen. Since the temperature changes are relatively slow thermal lag is not expected to play a significant role.

G. DIC analysis

Several alternatives for open-source (e.g., [17], [18], [19]) and commercial 2D- and stereo-DIC software have been

TABLE I. DIC HARDWARE AND SOFTWARE PARAMETERS FOR AN EXAMPLE CTE MEASUREMENT

Parameter [unit]	Value
Image filtering	Gaussian 5 px kernel
Reference image	Cumulative (Spatial)
Interpolation	Bi-cubic spline (Local)
Matching criterion	Zero-normalized sum-of-square differences
Mean Speckle size [px]	Approx 6.8
Image noise	Approx 1 % full scale
Subset size [px]	31
Step size [px]	5
Subset shape function	Quadratic
Strain Window	25
Strain formulation	Green-Lagrange modified quadratic (Q9)
Virtual strain gauge [px]	151

evaluated and tested, and a custom Python-based comparison suite was implemented to evaluate the options. Under ideal circumstances the software packages provide similar results, but performance differs under nonideal conditions. A full comparison is outside the scope of this work. For the (E)CS and CTE experiment example cases, a workflow based on the MatchID software package is used in accordance with the International Digital Image Correlation Society's Good Practices Guide [15].

For the DIC displacement and strain measurements, the following workflow is performed. First, images and calibration were imported into the software. Second, a circular region of interest (ROI) centered on the specimen is defined (e.g., see Fig. 2a). For effective cure shrinkage, a second ROI (not shown) is defined on the speckled backer sheet in an annulus surrounding the epoxy. Third, analysis parameters are selected. Fourth, an initial guess is determined. And fifth, the correlation and strain computations are conducted, and outputs are saved to .csv data files which provide an open data format for post-processing.

H. Post-processing and example CTE results

The analysis parameters are listed in Tab. I. To obtain the CTE from the DIC and thermocouple data, the DIC data .csv and thermocouple data .csv files are imported into post-processing scripts. Edges of the data are eroded using a 5 px disk structuring element to reduce the influence of edge effects typically seen in DIC analyses. Then, the Green-Lagrange Q9 strain fields ($\underline{\epsilon}_{ij_t}$) for each time step are spatially averaged (mean ± standard deviation) and the vector magnitude is computed for each time point. This strain $\left|\underline{\epsilon}_{ij_t}\right|$ is taken to be the surface strain associated with cure shrinkage and/or thermal strain. The measurement uncertainty is defined as the geometric sum of the noise floor and standard deviation of the strain from the spatial averaging, since the (E)CS and CTE strain fields are nominally homogeneous.

To compute CTE from the strain-temperature data in Fig. 2c a first order polynomial, i.e., linear model, is fit to the data

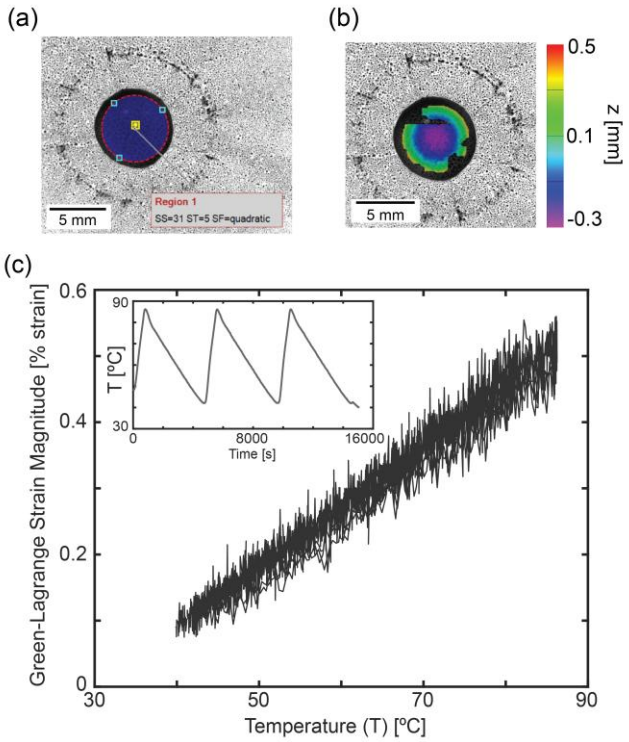

Fig. 2 Example DIC data for CTE measurement. (a) Snapshot of the DIC software showing the speckle pattern, ROI, and initial subset. (b) Example DIC result showing the out-of-plane shape measured with the stereo-DIC and plotted as a overlayed heatmap. (c) Primary CTE measurement data showing the strain versus temperature for the three-cycle measurement. Strain uncertainty is estimated to be ±0.13 % strain. *Inset.* The measured temperature of the aluminum test plate (note the actual surface temperature is several °C higher than nominal (one standard deviation ±0.08 °C).

during the three complete 40 °C to 75 °C cycles. A least-squares routine with least absolute residuals metric was used to compute the slope of the strain-temperature curve with a 0.99 confidence interval (CI). The slope of this line is the CTE. Since the surface strain is measured, the $\left|\underline{\epsilon}_{ij_t}\right|$ value is associated with the linear, rather than volumetric, CTE. For the example case, the data are highly linear ($R^2 = 0.965$), as expected for this material and temperature range. The measured CTE for the TM01 material with an 8 h, 120 °C cure was $\alpha = 89.9$ µstrain/K (0.99 CI: [89.1 µstrain/K, 90.7 µstrain/K]), which is consistent with values for similar unfilled epoxy reported elsewhere [20], [21].

III. CONCLUSION

This manuscript discussed a research platform used for the development of DIC-based metrology for semiconductor packing. It is implemented using a mix of commercial-off-the-shelf components and custom-designed parts. While this type of system has been used elsewhere to make similar measurements and may be commercially available as a turn-key solution, this work attempts to describe the development process in order to demystify the application of DIC metrology for measuring cure shrinkage and coefficient of thermal

expansion. While many other approaches exist, this also demonstrates that DIC can be a straightforward, inexpensive means to obtain data comparable to other techniques.

Looking ahead, additions include improved *in situ* calibration, coupled finite element model to address the influence of the backer sheet, and developing an *in situ* confinement rig to simulate the cure environment during underfilling.

DATA AVAILABILITY

Primary data associated with this paper are publicly available through the NIST Public Data Repository at https://doi.org/10.18434/mds2-4101 [22].

DISCLAIMER

Certain equipment, instruments, software, or materials are identified in this paper to specify the experimental procedure adequately. Such identification is not intended to imply recommendation or endorsement of any product or service by NIST, nor is it intended to imply that the materials or equipment identified are necessarily the best available for the purpose.

ACKNOWLEDGMENT

I thank Amanda Forster for assistance with project management and Andrew Korvich for preparation of the TM01 material. Shawn Chen assisted with development of the DIC comparison tool.

REFERENCES

[1] D. Lu and C. P. Wong, Eds., *Materials for Advanced Packaging*. Boston, MA: Springer US, 2009. doi: 10.1007/978-0-387-78219-5.

[2] R. Tao *et al.*, "Material needs and measurement challenges for advanced semiconductor packaging: understanding the soft side of science," *IEEE Transactions on Components, Packaging and Manufacturing Technology*, vol. 15, no. 10, pp. 2071–2082, Oct. 2025, doi: 10.1109/TCPMT.2025.3603484.

[3] S. P. Phansalkar, C. Kim, and B. Han, "Effect of critical properties of epoxy molding compound on warpage prediction: a critical review," *Microelectronics Reliability*, vol. 130, p. 114480, doi: 10.1016/j.microrel.2022.114480.

[4] C. Cai, H. Wang, J. Yang, P. Yin, and S. B. Park, "A comprehensive study on characterization of residual stress of build-up layer and prediction of chip warpage," *J. Electron. Packag*, vol. 146, no. 021006, doi: 10.1115/1.4063919.

[5] Y. Gao *et al.*, "In-situ measurement method for warpage of electronic package substrate based on speckle-free DIC and carbon coating," in *2025 26th International Conference on Electronic Packaging Technology (ICEPT)*, Aug. 2025, pp. 1–5. doi: 10.1109/ICEPT67137.2025.11157196.

[6] Y. He, B. E. Moreira, A. Overson, S. H. Nakamura, C. Bider, and J. F. Briscoe, "Thermal characterization of an epoxy-based underfill material for flip chip packaging," *Thermochimica Acta*, 2000.

[7] P. Y. Liao *et al.*, "Die bonding solution for flip chip-chip scale package-DIC (Digital Image Correlation) and Shadow Moiré application," in *2022 IEEE 72nd Electronic Components and Technology Conference (ECTC)*, May 2022, pp. 182–186. doi: 10.1109/ECTC51906.2022.00039.

[8] C. Jang, S. Yoon, and B. Han, "Measurement of the hygroscopic swelling Coefficient of thin film polymers used in semiconductor packaging," *IEEE Transactions on Components and Packaging Technologies*, vol. 33, no. 2, pp. 340–346, Jun. 2010, doi: 10.1109/TCAPT.2009.2038366.

[9] K. A. Deo, P. Yin, J. Yang, J. H. Ha, and S. B. Park, "A technical review on state of the Art In-Plane and Out-of-plane deformation measurement techniques for microelectronic packages," in *2023 IEEE 73rd Electronic Components and Technology Conference (ECTC)*, May 2023, pp. 907–913. doi: 10.1109/ECTC51909.2023.00305.

[10] *Package Warpage Measurement of Surface-Mount Integrated Circuits at Elevated Temperature*, JESD22-B112C, Nov. 01, 2023. Accessed: Jan. 30, 2026. [Online]. Available: https://www.jedec.org/standards-documents/docs/jesd-22-b112

[11] C. Cai, K. Pan, J. Yang, and S. Park, "Comparative analysis of package warpage using confocal method and Digital Image Correlation," in *2020 19th IEEE Intersociety Conference on Thermal and Thermomechanical Phenomena in Electronic Systems (ITherm)*, Jul. 2020, pp. 945–949. doi: 10.1109/ITherm45881.2020.9190235.

[12] P. Centellas *et al.*, "Advanced metrology suite for linking residual stress to fundamental properties of thermoset packaging materials," in *2025 IEEE 75th Electronic Components and Technology Conference (ECTC)*, IEEE, 2025, pp. 432–439. Available: https://ieeexplore.ieee.org/abstract/document/11038178/

[13] S. P. Phansalkar, C. Kim, B. Han, and P. J. Gromala, "Volumetric effective cure shrinkage measurement of dual curable adhesives by fiber Bragg grating sensor," *Journal of Materials Science*, vol. 55, no. 22, pp. 9655–9664, Aug. 2020, doi: 10.1007/s10853-020-04716-1.

[14] S. P. Phansalkar and B. Han, "Measurement of temperature-dependent viscoelastic compressibility of highly-filled thermosets using inert gas pressure," *Journal of the Mechanics and Physics of Solids*, vol. 199, p. 106087, Jun. 2025, doi: 10.1016/j.jmps.2025.106087.

[15] Jones, E.M.C. and Iadicola, M.A. (Eds.), "A Good Practices Guide for Digital Image Correlation, Edition 2." International Digital Image Correlation Society, 2025. [Online]. Available: https://doi.org/10.32720/idics/gpg.ed2

[16] W. S. LePage, S. H. Daly, and J. A. Shaw, “Cross polarization for improved Digital Image Correlation,” *Experimental Mechanics*, vol. 56, no. 6, pp. 969–985, Jul. 2016, doi: 10.1007/s11340-016-0129-2.

[17] D. Z. Turner, “Digital Image Correlation Engine (DICe) Reference Manual,” SAND2015-10606 O, 2015.

[18] D. Solav, K. M. Moerman, A. M. Jaeger, K. Genovese, and H. M. Herr, “MultiDIC: An open-source toolbox for multi-view 3D Digital Image Correlation,” *IEEE Access*, vol. 6, pp. 30520–30535, 2018, doi: 10.1109/ACCESS.2018.2843725.

[19] A. K. Landauer, M. Patel, D. L. Henann, and C. Franck, “A q-factor-based Digital Image Correlation algorithm (qDIC) for resolving finite deformations with degenerate speckle patterns,” *Experimental Mechanics*, vol. 58, no. 5, pp. 815–830, Jun. 2018, doi: 10.1007/s11340-018-0377-4.

[20] M. Sadeghinia, K. M. B. Jansen, and L. J. Ernst, “Characterization and modeling the thermo-mechanical cure-dependent properties of epoxy molding compound,” *International Journal of Adhesion and Adhesives*, vol. 32, pp. 82–88, Jan. 2012, doi: 10.1016/j.ijadhadh.2011.10.007.

[21] L. Khoun, T. Centea, and P. Hubert, “Characterization methodology of thermoset resins for the processing of composite materials — case study: CYCOM 890RTM epoxy resin,” *Journal of Composite Materials*, vol. 44, no. 11, pp. 1397–1415, Jun. 2010, doi: 10.1177/0021998309353960.

[22] P. Centellas, R. Tao, A. Korovich, and A. Landauer, “Data for controlling the reaction pathway to tune packaging epoxy properties.” NIST Public Data Repository. doi: https://doi.org/10.18434/mds2-4101.